

Granular Segregation in Tapered Rotating Drums

S. González^{1,*} and L. Orefice¹

¹Research Center Pharmaceutical Engineering GmbH, Inffeldg. 13, Graz, Austria

We study the granular segregation in a tapered rotating drum by means of simulations. In this geometry, both radial and axial segregation appear, the strength of which depends on the filling fraction. We study the effect of the drum's tapering angle on the segregation speed and show that, coherently with several recent studies, the axial segregation is due to the combined effect of the radial segregation and the shape of the drum. We show that the axial segregation behaves in a way analogous to the one found in chute flows, and corresponds to previous theories for shallow gravity driven surface flows with diffusion. By means of this analogy, we show that tapered drums could be the simplest experimental set-up to obtain the free parameters of the theory.

PACS numbers: 45.70.Mg

It has been hinted that axial segregation in rotating drums is mainly the result of the shape of the free-surface, the thin layer of flowing particles in the drum [1–4]. The free-surface is not flat, but slightly curved along the axial direction, with peaks near the parallel walls of the drum. Due to the friction with them, the particles on the sides are lifted more than the particles in the centre, thus creating a convective flow in the drum that induces the axial segregation. How to harvest this relation between flow and the segregation pattern remains an open question: a question whose answer could have far-reaching practical implications.

Motivated by the results of [5, 6] – where axial segregation of binary mixtures in a tapered rotating drum is reported albeit not explained – and how they relate to our own results [7] – where the shape of the rotating drum is used to speed up and control the axial segregation – we study the segregation pattern in tapered rotating drums by means of simulations, and see to what extent it is possible to control it by modifying the drum's shape.

It has recently been shown that, contrary to the common belief that 3D rotating drums are the sum of independent quasi-2D slices interacting only via diffusion, the shape of the drum does influence the surface flow creating a slow axial drift [3]. This drift is caused by the axial slope of the drum's walls, which determines the 3D structure of the flow. If a bi-disperse mixture is used, the particles will follow the flow structure and will segregate accordingly.

In the particular case of a tapered drum, when mixed particles enter the flowing layer in the upper part of the avalanche, gravity drives them towards the small side of the drum before returning them to the large one. Small particles can percolate through the voids created by the big ones leaving the flowing layer before it changes its direction. This leads to a net transport of small particles to the small side of the drum and of large particles to the big side: axial segregation occurs. Since the shape of the flowing layer depends on the shape of the drum, one would also expect it to affect the segregation. In this paper we show that this is indeed the case and we study how it happens.

The coupling of axial segregation with the velocity profile has been already reported for the classical rotating drum [4]. In the tapered rotating drum the same coupling is in play

but with a fundamental difference: the shape of the drum increases the curvature of the flow lines on the flowing layer thus transporting more small particles than in a parallel drum, and in contrast to the latter, *in a definite direction*.

The structure of the paper is as follow. First, the drum geometry and simulation details are explained. Second, we compare our results for half-filled drums with experiments to validate our model. Third, to minimize the effect of radial segregation, a lower filling fraction is used and total segregation is observed. The effect of the drum's tapering angle on the speed of the segregation is also studied. Finally, comparisons will be drawn with simulations of mixtures in 2 and 3D chutes and with a theory for shallow gravity driven surface flows with diffusion.

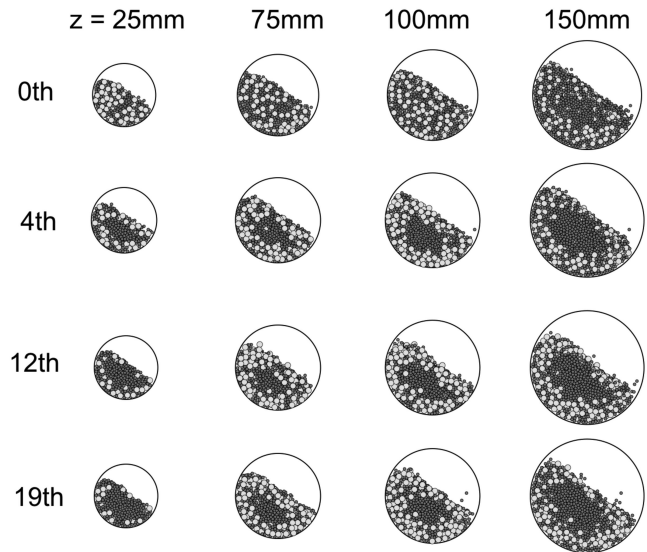


FIG. 1: (Color online) Snapshots for half-filled system at different positions along the rotation axis (from left to right) and different times (from top to bottom, the number of revolutions indicated in the left). Small particles dark, large particles light. One can see that first the radial segregation appears, and this slowly and continuously transforms into axial segregation, that here is visible in the dominance of small particle in the small side of the drum.

SIMULATIONS

Our simulations are in a slightly different geometry than that of [5, 6] (shorter drum) to speed up the simulation time. We use an equal volume mixture of 5 and 10mm radii particles in a tapered drum 150mm length, with caps of radii $r = 50$ mm (at $z = 0$ mm) and variable R (at $z = 150$ mm), in the left and right side, respectively. Their relation define the angle of the drum, such that $R = r(1 + \tan(\alpha))$. In the simulations, particles' contact forces are represented using a standard spring dash-pot model [8] as implemented in [9]. The angular velocity is set to $\pi \text{ s}^{-1}$, i.e. 30rpm, which implies an average Froude number of $Fr = \omega^2(r+R)/2g \sim 0.1$. The system is either at 50 or 25% filling fraction. As initial condition the particles are arranged in a square lattice, alternating one big particle and eight small to obtain an initial mixed state. Snapshots of the system for different times and axial positions are shown in Fig. 1 (cf. Fig. 5 in Ref. [6] for an experimental comparison).

The simulations were performed using Mercury-DPM [9] with the same material properties used in our previous research [7], since they proved to reproduce the experimental results.

Shape of the Free Surface

In this section we show the three-dimensional structure of the flow. We focus on three different characteristics: the level of the surface along the axis of rotation (Fig. 2), the velocity field on the free surface (Fig. 3) and the density profile, as seen by a vertical cut in the centre of the drum (Fig. 4). Together, they provide a rather complete way to visualise the structure. Data are averaged for 30 consecutive snapshots (one every 0.8s) and coarse-grained to obtain a continuous function following the procedure of Ref. [10]. The weight function is a Lucy polynomial [11] with a width of $2d$. Unless otherwise noted, every coarse-graining presented here is done with the same parameters. We measured at different times during the evolution of the system, and the results do not significantly change, so we conclude that what we observe depends only on the geometry and not in the degree of segregation.

The free surface along the axial direction shows level differences. This phenomenon, to the best of our knowledge, was first described by Zik et al. for a drum modulated along the axial direction with a sinusoidal function [12]. This can be seen in our simulations from Fig. 1, or looking at the iso-lines of the density at different axial positions, in Fig. 2. This level difference along the axis makes particles to move along the gradient of the surface, that is as particles go down the avalanche, they move forwards and backwards in the axis perpendicular to the page.

Particles enter the flowing layer with a small velocity and they are mainly directed towards the small side of the drum. This is due to the tapered geometry: when entering the flowing layer, the particles in the large side of the drum are higher than those in the small side of the drum, thus creating a flow

towards the small side. This is inverted when particles reach the lower part of the avalanche: particles in the large side of the drum are lower than those in the small side. Increasing the angle of the drum, increases the curvature and the magnitude of this flow. This can be seen in Fig. 3 for three different angles. The surface is defined as the plane whose projection can be seen in Fig. 2 (solid line).

When a mixture of particles enters the avalanche in the upper part, they will segregate as they travel downslope. If the drum is large enough, some small particles will reach the core before the flow changes its direction, creating a net transport of small particles. (Large enough here means in relation to the segregation speed of the mixture. For size-driven segregation, the smaller the size ratio of the particles, the slower segregation is, and thus the drums needs to be larger.) The large particles, since they tend to stay on the surface, can flow back to the large side of the drum, following the flow lines. In this way, axial segregation occurs.

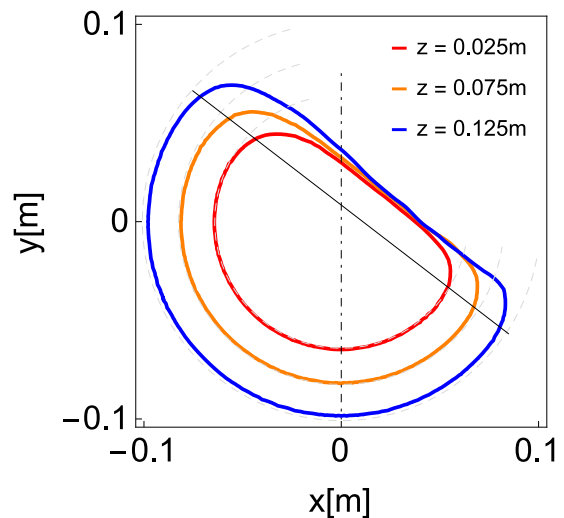


FIG. 2: Contour lines for a density $\rho^* = \rho_{particles}/10$ at three different axial positions for the same systems as in Fig. 1. The level difference can be seen mostly in the upper part of the avalanche. One should think of the curves as being displaced in the direction normal to the page. Compare the qualitative agreement with the model of Ref. [12]. Note that since the flow velocity increases along z , the blue curve shows a slightly more S-shaped profile. Solid line shows the plane where the velocity is measured for Fig. 3 and dashed vertical line the plane where the density is measure for Fig. 4.

Finally, the packing fraction of the system gives us an insight on the inner structure of the flow, and shows the dependence of the free surface on the drum's angle, Fig. 4. Despite the presence of segregation, the density is uniform during the evolution of the system, with the densest region at the bottom of the drum. The density is mostly homogeneous along the axial direction with increased spatial fluctuations as α increases.

The density remains constants during the segregation process, and is maximum in the lower region of the drum for all the angles studied. We confirmed that the density does not

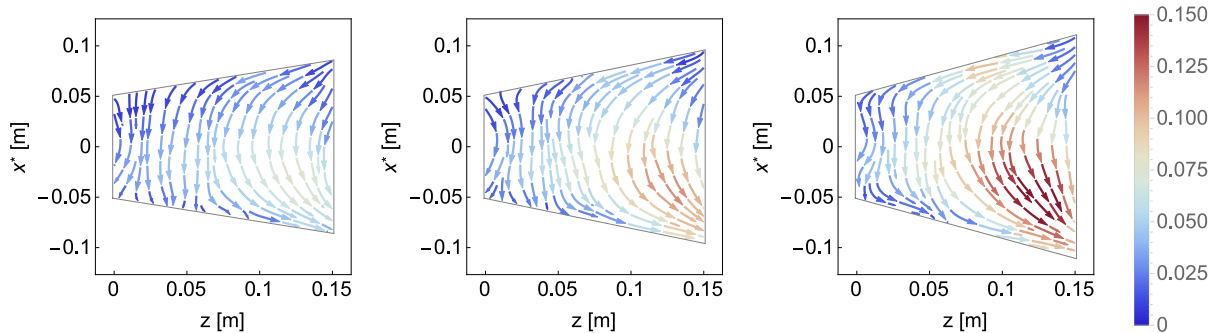


FIG. 3: Average velocity field of the particles' free surface for the tapered drum (from left to right, tapering angle $\alpha = 10^\circ, 15^\circ, 20^\circ$), the colour representing the particles' mean velocity in m/s . The length of the component of the vector field parallel to the axis of rotation is increased to stress the effect of the tapered geometry on the flow. As expected, the convective flows increases its amplitude and reach with the angle of tapering.

vary by measuring it at different times during the segregation process.

Radial and Axial Segregation

To corroborate that the proposed mechanism is responsible of the axial segregation, we measure the radial and axial segregation in the drum as a function of time. In order to have order parameters for both, the radial segregation is defined as follows:

$$q_{\text{radial}} = N_{s < z^*} / N_{Ts} + N_{L > z^*} / N_{TL} - 1, \quad (1)$$

where $N_{s < (L >) r^*}$ is the number of small (large) particles whose radial coordinate is smaller (larger) than the half volume radius r^* (note that this radius depend on the axial coordinate), $N_{Ts(L)}$ being the total number of small (large) particles. That is, we count the fraction of particles that are in the expected side of the drum. When $q_{\text{radial}} = 1$ all the large particles are in the outside and the small in the core of the drum. It must be noted that, due to the flowing layer, the radial segregation can never reach the maximum value. To measure the axial segregation we use a quantity that also works with banding (which appeared in one of the systems studied) [13]:

$$q_{\text{axial}}(t) = \frac{1}{l} \int_0^l \frac{|c_s(z, t) - \bar{c}_s(z)|}{\bar{c}_s(z)} dz, \quad (2)$$

where $c_s(z, t)$ is the number of small particles along the axis, and $\bar{c}_s(z)$ the number of small beads that correspond to a slice of the drum at position z for the totally mixed state. It must be noted that since we are simulating a tapered rotating drum, the mean number of small particles changes with z since the cross section of the drum increases accordingly.

Figure 5 shows the temporal evolution for each kind of segregation for three different angles. As expected, the radial segregation sets in quite fast, essentially after four turns, but it

saturates soon to a roughly constant value. On the other hand, the axial segregation is slower but steadily increases beyond the point of saturation for the radial segregation. Eventually (around the 10th revolution) the axial segregation causes the value of q_{radial} to decrease slightly, since in the small side of the drum the number of large particles decreases greatly.

If α is increased the segregation speed should increase since the level difference on the free surface is also increasing [12]. This is indeed the case as [5] shows experimentally (see in particular Fig. 8). The same principle can be seen in other configurations such as the spherical drum [14], or the double cone configuration [15].

To better understand the role of geometry on the segregation process, several simulations were run for different α . It is expected that the radial segregation will not depend on the geometry of system. However, for the axial segregation, since it depends on the velocity profile and on the geometry of the flowing layer, one expects to find a strong dependence on the angle of the drum since this determines the level difference in the flow. Indeed this is the case as Fig. 5 shows.

Less than Half Filled Drum

Our previous result shed light on the relation between α and the axial segregation, but this is strong influenced by the radial segregation in half filled drum. So large in fact, that at this filling fraction some systems segregate the other way around, that is, large particles in the small side of the drum, as reported in [5] and confirmed by some of our simulations (data not shown). We ran simulations at 25% filling fraction, for different α , and we observe indeed that the axial segregation is bolder. What is more, the radial segregation disappears almost completely since the mixing at this filling fraction is maximum [16]. In this configuration, a pure phase of small particles appears in the small side of the drum and a steady state for the segregation is reached, while increasing the angle of the drum increases the segregation speed (see Fig. 6).

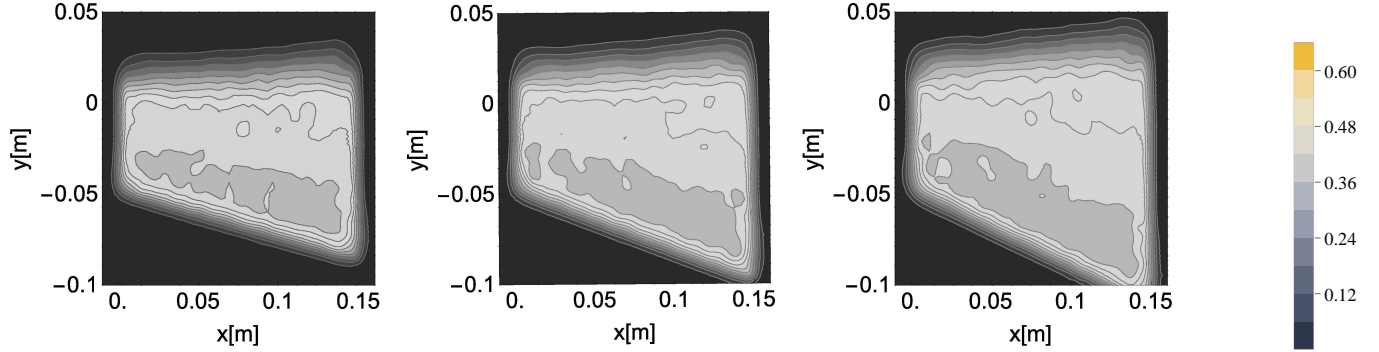


FIG. 4: (Color online) Packing fraction on the middle plane of the drum for increasing drum angles $\alpha = 10^\circ, 15^\circ, 20^\circ$, from left to right. The increasing slope of the free surface can be seen from left to right, as α increases.

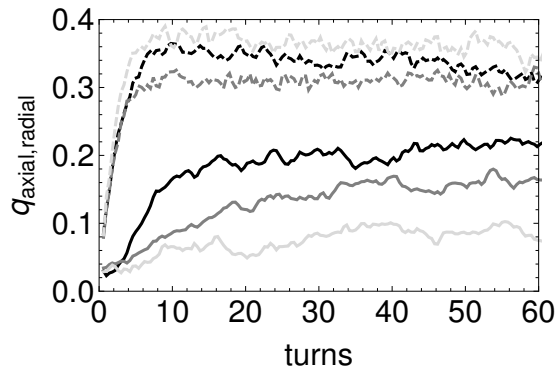


FIG. 5: Axial (solid-lines) and radial (dashed-lines) segregation as a function of time for the tapered rotating drum. From light gray to black in increasing angle of tapering. As it can be seen, there is no correlation between the angle and the radial segregation. However, axial segregation shows a clear correlation with α .

This behaviour is strikingly similar to that of bi-disperse chute flows, either in 2D [17] or 3D [18]. Numerically, those are simulated with a box with periodic boundary conditions in the flowing plane, and a rough inclined bottom. Depending on the inclination of the bottom with respect to gravity, a steady flow can be obtained. This is a straightforward way to study segregation for a fixed velocity profile, however their experimental realisation is rather complex.

Figure 6 shows the displacement of the centre of mass of the large particles normalized by its asymptotic value, for three different drum angles

$$\Delta z = \frac{z_{cm}(\infty) - z_{cm}(t)}{z_{cm}(\infty) - z_{cm}(0)}, \quad (3)$$

where $z_{cm}(t)$ is the centre of mass position on the axial direction for the large particles. As α increases, the system segregates faster since the shear rate increases with it. One can see that the drum's angle influences the segregation in the same

way as the size ratio between the particles [18, 19] or the volume fraction between the two species [17].

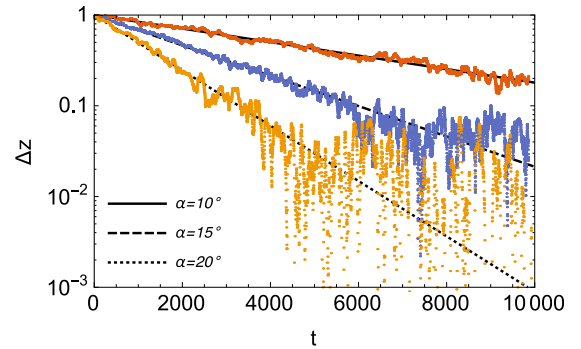


FIG. 6: Displacement of the centre of mass of large particles for systems with different α , normalized by the asymptotic value Δz in a log-linear scale. Straight lines correspond to the exponential fit. Compare with Ref. [17]. If plotted in a linear scale, one obtains results as in Ref. [18].

This is valid for a wide range of drum angles. We define the segregation speed as the inverse of the exponent of the exponential fit $\Delta z = \exp(-t/\tau)$. In general, the segregation speed is a monotonic function of the angle, as one can see in Fig. 7, the line being a linear eye-guide. A simple estimation tells us that the distance a particle travels on the free surface is $L_s \propto \tan(\alpha)$. If the particles travel twice as much during one avalanche they will segregate twice as fast, and this would explain the linear behaviour of the segregation speed with the angle.

Since we have this qualitative agreement between two completely different systems, the obvious next step is to see how well the theoretical predictions developed for the chute flow work on the tapered drum.

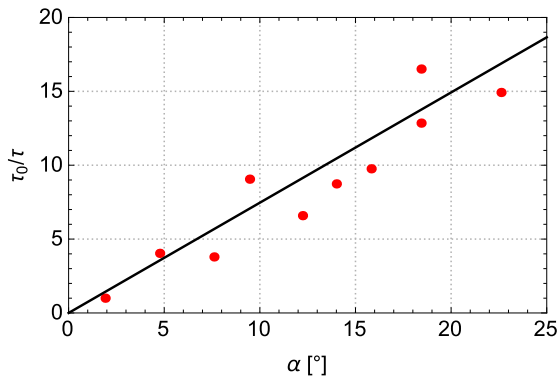


FIG. 7: Normalised segregation speed measured as the inverse of the typical time, τ_0/τ obtained from the centre of mass displacement on Fig. 6 for different tapering angles (τ_0 is the typical time for $\alpha = 2^\circ$). The solid line is a linear eye guide.

Comparison with theory

Let us look at the phenomenon from another point of view. Since the free surface is at an angle with respect to the horizontal (going up towards the large side of the drum, see Fig. 2) the projection of gravity on the free surface is non-zero. This translates into an effective gravity towards the small side of the drum. From the theory for shallow granular avalanches [20, 21] we know the time evolution for the concentration of each species, and we should be able to apply this result to the tapered drum.

Whereas the chute flow develops vertical segregation as it moves downslope, the rotating drum develops axial segregation as time passes. This is due to the structure of the flow as seen in Fig. 3. The tapered drum turns the kinetic sieving along the flow lines into axial segregation at the system's level. According to this simple analogy, small particles should go to the small side of the drum, while large particle will go towards the large side. Furthermore, since the free-surface is a geometric characteristic of the flow and does not depend on the degree of segregation of the mixture, the tapered drum will segregate the particles into stable configurations in the same manner that a chute flow does.

The temporal evolution of the concentration is something particularly difficult to measure experimentally and, to the best of our knowledge, there is only one realisation [22]. Our results show a strikingly good fit with the theory, Fig. 8. For the sake of space, we refer the reader to the original paper for the derivation of the solution [23] and to the appendix for the explicit formula we use. Note that for a tapered drum the half volume height is at $z_{50} = L/\sqrt{2}$, the spatial coordinate of the theoretical solution has been scaled to account for this.

The results are remarkably similar concerning both the evolution of the concentration and the spatial distribution. However, we cannot fit both the temporal evolution and the steady state solution. We chose to fit the Péclet number Pe (a dimensionless number that quantifies how large the segregation is

compared to diffusive remixing) to reproduce the evolution of the system rather than the steady state. Does this mean that the Pe in the tapered drum changes with time? Answering this question goes beyond the scope of this paper.

It must be noted that we are comparing the results of only one realisation, and our data points are not averaged on time, which would decrease the noise and give a better fit, but we prefer to show the raw results to highlight the quality of the data that is possible to obtain with this set-up. We confirmed that the same qualitative behaviour holds for different angles and drum lengths (data not shown).

Finally, it must be noted that Gray & Chugonov's theory can be used to explain the centre of mass movement reported in [17, 18], together with our results. Consider the solution for the concentration of small particles in the chute, $\phi(x, t)$. To obtain the centre of mass of the small particles one integrates the concentration times the position, $z_{cm}(t) = \int_0^1 z \phi(z, t) dz$, which can be solved numerically in a very straightforward way. It is easy to verify that the predicted solution shows an exponential decay for small values of $Pe \sim 4$, but seems to show two different slopes for larger values of it. In this way, Pe can be measured not only for the steady state solution, as done in [18] but from the evolution of the system. The results presented here indicate that both may be different.

A detailed study of Pe for different system parameters is beyond the scope of this paper. Our objective being to show how well the theory describe the evolution of the system and how the tapered drum could become a trivial experimental set-up where to measure the Péclet number. A detailed study of this should be hopefully a subject to be addressed both experimentally and theoretically in the future.

CONCLUSIONS

We have studied the size-driven segregation of bi-disperse mixtures in tapered rotating drums. The relation between velocity field, free surface, and the segregation pattern was studied. The results confirm that level differences on the free surface create axial flows, which in turn cause axial segregation. For the first time we report total axial segregation in this particular geometry and we studied its dependence on different parameters; in particular, we showed that the axial segregation speeds up with the angle of the drum.

We have shown that tapered drums can be used to determine the Péclet number used in previous theories from a straightforward experimental set-up. This has been done before but the experiments are very difficult to set up "with both well controlled initial conditions and a steady uniform bulk flow field" [22]. And indeed, to the best of our knowledge, the results from Wiederseiner et al. are the only ones that give the Péclet number experimentally. On the contrary, to obtain well controlled results on a tapered drum is extremely easy, for example, using the same set-up that motivated this study [5].

Besides these theoretical implications, the results presented

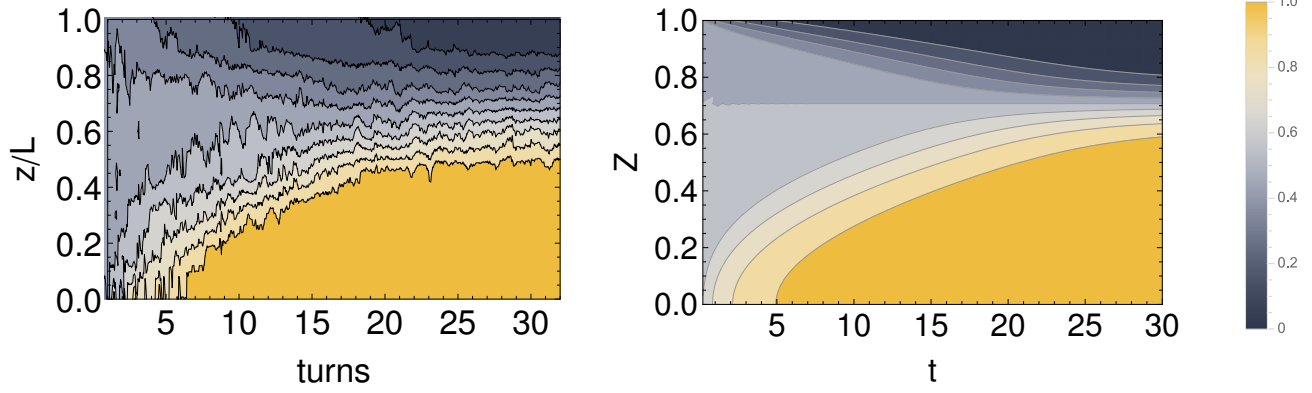


FIG. 8: Left panel, concentration of small particles along the normalized rotation axis as a function of time for our numerical experiments with $\alpha = 10^\circ$ and $L = 200\text{mm}$. Right panel, theoretical solution using the results of Ref. [23] with $Pe = 14$.

here have direct applications in the separation and sorting of granulates in areas ranging from powder handling in the pharmaceutical industry to ore milling in the mining industry and shed light on the important role of geometry in segregation processes, not only for rotating drums but everywhere tridimensional flows appear.

ACKNOWLEDGMENTS

This work was supported by the IPROCUM Marie Curie initial training network, funded through the People Programme (Marie Curie Actions) of the European Union's Seventh Framework Programme FP7/2007-2013/ under REA grant agreement No. 316555. We would like to thank J. Kihnast, N. Rivas, W. den Otter, S. Luding and A.R. Thornton for fruitful discussions, and the kind hospitality of A. Michrafy at the Ecole de Mines, Albi, France, where part of work was realised. The simulations performed for this paper were undertaken in Mercury-DPM. It is primarily developed by T. Weinhart, A.R. Thornton and D. Krijgsman at the University of Twente.

Appendix I

The general solution for the concentration of small particles can be written as

$$\phi = \frac{1}{2} \left(1 - \frac{2}{\omega} \frac{\partial \omega}{\partial \xi} \right),$$

where ω is decomposed onto a steady and a time-varying part $\omega = \omega_s + \omega_\tau$. Their analytical forms is given by

$$\omega_s = \chi_0(\xi_0) \frac{\sinh(\xi/2)}{\sinh(\xi_0/2)} - \frac{\sinh((\xi - \xi_0)/2)}{\sinh(\xi_0/2)},$$

for the steady solution, while the temporal part is given by

$$\omega_\tau = \sum_{n=1}^{\infty} A_n \exp\left(-\left(\frac{n^2 \pi^2}{\xi_0^2} + \frac{1}{4}\right)\tau\right) \sin\left(\frac{n\pi\xi}{\xi_0}\right).$$

where the transformed time and space variables are given by $\tau = (S_r^2/D_r)t$ and $\xi = (S_r/D_r)z$ and $\xi_0 = Pe$. For an equal volume mixture, as in our case, $\chi_0(\xi_0) = 1$. Using Eq. (5.46) from [23] for our mean concentration $\phi_m = 0.5$, we find that the coefficients in the Fourier sine series are simplified into

$$A_n = \frac{2Pe^2}{n\pi(Pe^2 + 4n^2\pi^2)} (1 - (-1)^n).$$

In our solution, we take only the first hundred terms of the series.

* s.gonzalez@tugraz.at

- [1] M. M. H. D. Arntz, W. K. Otter, H. H. Beefink, R. M. Boom, and W. J. Briels, *Granular Matter* **15**, 1 (2012).
- [2] N. A. Pohlman and D. F. Paprocki Jr., *Granular Matter* **15**, 1 (2012).
- [3] Z. Zaman, U. D'Ortona, P. B. Umbanhowar, J. M. Ottino, and R. M. Lueptow, *Phys. Rev. E* **88**, 012208 (2013).
- [4] P. Chen, J. M. Ottino, and R. M. Lueptow, *New Journal of Physics* **13**, 055021 (2011).
- [5] T. Kawaguchi, K. Tsutsumi, and Y. Tsuji, *Particle & Particle Systems Characterization* **23**, 266 (2006).
- [6] H. Yada, T. Kawaguchi, and T. Tanaka, *Flow Measurement and Instrumentation* **21**, 207 (2010).
- [7] S. Gonzalez, C. R. K. Windows-Yule, S. Luding, D. J. Parker, and A. R. Thornton, *ArXiv e-prints* (2014), 1410.6286.
- [8] P. A. Cundall and O. D. L. Strack, *Géotechnique* **29**, 47 (1979).
- [9] A. R. Thornton, T. Weinhart, S. Luding, and O. Bokhove, *International Journal of Modern Physics C* **23**, 1240014 (2012).
- [10] T. Weinhart, A. R. Thornton, S. Luding, and O. Bokhove, *Granular Matter* **14**, 289 (2012).
- [11] L. B. Lucy, *The astronomical journal* **82**, 1013 (1977).

- [12] O. Zik, D. Levine, S. G. Lipson, S. Shtrikman, and J. Stavans, *Phys. Rev. Lett.* **73**, 644 (1994).
- [13] N. Taberlet, W. Losert, and P. Richard, *EPL (Europhysics Letters)* **68**, 522 (2004).
- [14] L. Naji and R. Stannarius, *Phys. Rev. E* **79**, 031307 (2009).
- [15] A. W. Alexander, T. Shinbrot, and F. J. Muzzio, *Physics of Fluids* **13**, 578 (2001).
- [16] G. Metcalfe, T. Shinbrot, J. J. McCarthy, and J. M. Ottino, *Nature* **374**, 39 (1995).
- [17] L. Staron and J. C. Phillips, *Physics of Fluids* **26**, 033302 (2014).
- [18] A. Thornton, T. Weinhart, S. Luding, and O. Bokhove, *International Journal of Modern Physics C* **23**, 1240014 (2012).
- [19] B. Marks, P. Rognon, and I. Einav, *Journal of Fluid Mechanics* **690**, 499 (2012).
- [20] J. M. N. T. Gray and A. R. Thornton, *Proc. Royal Soc. A* **461**, 1447 (2005).
- [21] J. M. N. T. Gray and C. Ancey, *Journal of Fluid Mechanics* **678**, 535 (2011).
- [22] S. Wiedersseiner, N. Andreini, G. Épely-Chauvin, G. Moser, M. Monneréau, J. M. N. T. Gray, and C. Ancey, *Physics of Fluids* **23**, 013301 (2011).
- [23] J. M. N. T. Gray and V. A. Chugunov, *Journal of Fluid Mechanics* **569**, 365 (2006), ISSN 1469-7645.